

# Observation of fragile-to-strong liquid transition in surface water in $\text{CeO}_2$

E. Mamontov<sup>a)</sup>

*NIST Center for Neutron Research, National Institute of Standards and Technology, Gaithersburg, Maryland 20899-8562 and Department of Materials Science and Engineering, University of Maryland, College Park, Maryland 20742-2115*

(Received 1 August 2005; accepted 26 September 2005; published online 28 October 2005)

A quasielastic neutron-scattering experiment carried out on a backscattering spectrometer with sub- $\mu\text{eV}$  resolution in the temperature range of 200–250 K has revealed the dynamics of surface water in cerium oxide on the time scale of hundreds of picoseconds. This slow dynamics is attributed to the translational mobility of the water molecules in contact with the surface hydroxyl groups. The relaxation function of this slow motion can be described by a slightly stretched exponential with the stretch factor exceeding 0.9, which indicates almost a Debye-type dynamics. Down to about 220 K, the temperature dependence of the residence time for water molecules follows a Vogel-Fulcher-Tamman law with the glass transition temperature of 181 K. At lower temperatures, the residence time behavior abruptly changes, indicating a fragile-to-strong liquid transition in surface water at about 215 K. © 2005 American Institute of Physics. [DOI: 10.1063/1.2125729]

## I. INTRODUCTION

While dozens of quasielastic neutron scattering (QENS) experiments have investigated the dynamics of water confined in matrices with three-dimensional pores, quasi-two-dimensional surface water has received little attention. A possible reason is that, owing to their macroscopically large penetration depth, neutrons have been traditionally considered a bulk rather than a surface probe. However, the exceptionally large incoherent scattering cross section of hydrogen compared to other elements makes studies of surface water possible in the systems where the elements with low incoherent scattering cross section form small crystallites with sufficient cumulative surface area.

A few systems where the mobility of surface water has been investigated using QENS include  $\text{Cr}_2\text{O}_3$  (Ref. 1),  $\text{SrF}_2$  and  $\text{ZnO}$  (Ref. 2), and  $\text{ZrO}_2$  (Refs. 3 and 4). It has been observed that the dynamics of either a monolayer<sup>1,2</sup> or the outermost layer<sup>3</sup> of the surface water exhibits an Arrhenius-type temperature dependence, whereas a non-Arrhenius behavior has been found for the dynamics of the inner hydration layer.<sup>4</sup>

For the present study of surface water we have chosen nanocrystalline cerium oxide as a matrix. In  $\text{CeO}_2$ , the surface OH groups coordinated to one, two, or three surface cations are observed,<sup>5</sup> whereas in  $\text{ZrO}_2$  only one- and three-coordinated surface OH groups are present.<sup>6,7</sup> More importantly, in this work we have ventured into the low-temperature region down to 200 K, where supercooled water confined in three-dimensional pores of nanoporous silica has been recently demonstrated to exhibit a liquid transition from high-temperature “fragile” non-Arrhenius to low-temperature “strong” Arrhenius behavior<sup>8</sup> in agreement with a well-known prediction.<sup>9</sup> We observe that at  $\approx 215$  K sur-

face water in  $\text{CeO}_2$  exhibits a sudden change in its dynamics indicative of fragile-to-strong liquid transition.

## II. EXPERIMENT

Cerium oxide powder sample with a specific surface area of  $55 \text{ m}^2/\text{g}$  was purchased from Alfa Aesar. As-received powder was annealed in air at 773 K in order to ensure the removal of any organic residue from the surface without degrading the surface area. IR measurements of the powder were performed with a Thermo Nicolet Nexus 670 Fourier-transform infrared (FTIR) spectrometer having a resolution of  $4 \text{ cm}^{-1}$ . The IR spectra indicated the presence of molecular surface water. The thermal gravimetric analysis (TGA) measurements of the powder in the temperature range of 300–573 K showed a weight loss of 1.5%. The TGA measurements were repeated three times following the full recovery of the initial weight by the sample stored overnight under ambient conditions and demonstrated reproducibility and reversibility of the weight loss. The FTIR spectra collected prior to the TGA measurements and after the sample has regained its weight were practically identical. Thus, the reversible weight loss was attributed to molecular water. This attribution allows one to calculate the surface molecular water content to be 0.15 mole/mole of  $\text{CeO}_2$ , which corresponds to 9.3 water molecules per  $100 \text{ \AA}^2$  of the surface. One can estimate the surface coverage of about two layers assuming that 4.6  $\text{H}_2\text{O}$  molecules cover a fully hydroxylated surface of  $100 \text{ \AA}^2$ , as found for OH species in silica.<sup>10</sup> Similar molecular water coverage was found to form under ambient conditions in  $\text{ZrO}_2$  (Ref. 3).

Water-containing cerium oxide powder was placed in a thin annular aluminum sample holder chosen to ensure greater than 90% neutron beam transmission through the sample. The sample was sealed with an indium O ring and mounted onto the cold stage of a closed-cycle refrigerator, the temperature of which was controlled within  $\pm 0.1$  K.

<sup>a)</sup>Author to whom correspondence should be addressed. Fax: (301) 921-9847. Electronic mail: mamontov@nist.gov

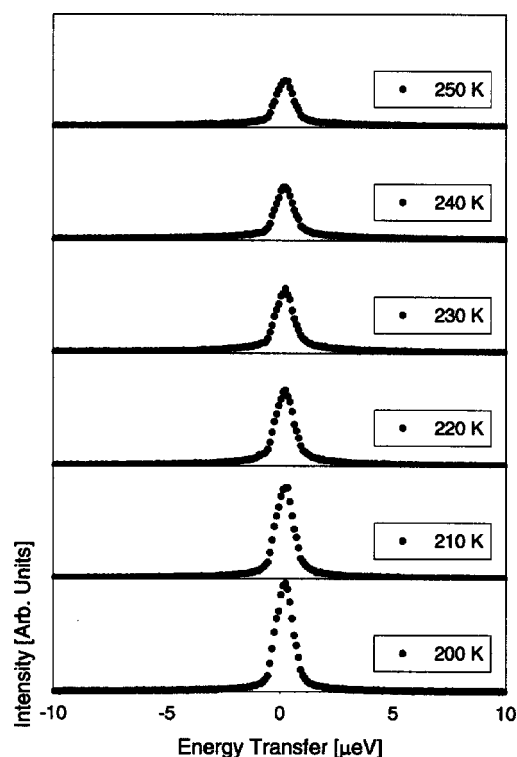


FIG. 1. The scattering intensities measured in the energy space at  $Q = 1.60 \text{ \AA}^{-1}$ . The data are plotted using the same scaling of the ordinate axes at each temperature point.

QENS experiment was performed using the high-flux backscattering spectrometer<sup>11</sup> (HFBS) at the National Institute of Standards and Technology (NIST) Center for Neutron Research. The incident neutron wavelength at the HFBS is varied via Doppler shifting about a nominal value of  $6.271 \text{ \AA}$  ( $E_0 = 2.08 \text{ meV}$ ). After scattering from the sample, only neutrons having a fixed final energy of  $2.08 \text{ meV}$  are measured by the detectors as ensured by Bragg reflection from analyzer crystals. The instrument was operated with a dynamic range of  $\pm 11 \text{ } \mu\text{eV}$  to provide the best energy resolution and the highest neutron counting rates. With this dynamic range, full width of the sample-dependent instrument resolution function at half maximum was  $0.85 \text{ } \mu\text{eV}$ , as measured with the vanadium standard. The data collected at 10 detectors ( $0.62 \text{ \AA}^{-1} < Q < 1.60 \text{ \AA}^{-1}$  at the elastic channel) were used in the data analysis. The QENS spectra were measured at 250, 240, 230, 220, 210, and 200 K. Independently collected vanadium spectrum was used as the instrument resolution function. An alternative approach, which could also provide additional information on the amount of signal due to the rapid water motions, would be to measure the resolution function from the sample cooled down to low temperatures where the water mobility has ceased.

### III. RESULTS AND DISCUSSION

The data collected at  $Q = 1.60 \text{ \AA}^{-1}$  are shown in Fig. 1 as an example. The spectra exhibit a quasielastic signal due to mobile water molecules. The width of the quasielastic wings is small compared to the dynamic range of the experiment even at the highest-temperature point of 250 K. In addition

to the quasielastic signal from the mobile water molecules, the spectra demonstrate a strong elastic line due to the surface hydroxyl groups, and possibly, water molecules that are immobile on the time scale of the experiment. It should be noted that the incoherent neutron-scattering cross section is zero for both cerium and oxygen. Thus, except for the  $Q$  values corresponding to the Bragg peaks, the contribution from the  $\text{CeO}_2$  matrix (mainly due to unknown impurities in cerium oxide) should be very small. The elastic intensity appears to grow rapidly below 220 K. Following the subtraction of the fitted linear background term, the data were Fourier transformed into the time space. The Fourier transformation could be applied to the data without introducing a significant termination error thanks to a small width of the quasielastic signal that decays to zero at the extremes of the dynamic range. Without subtraction of the fitted background, however, the data distortion in the time space would be pronounced at the short times. Since convolution with the resolution function in the energy space is replaced by a simple multiplication in the time space, the resulting scattering intensities in the time space were then divided by the Fourier-transformed resolution function yielding the intermediate scattering functions  $I(Q, t)$ . For the data analysis we have employed the model previously used in the study of the mobility of surface water in  $\text{ZrO}_2$  (Ref. 4):

$$I(Q, t) = x(Q) + y(Q) \exp \left[ - \left( \frac{t}{\tau} \right)^\beta \right], \quad (1)$$

where the term  $x(Q)$  originates from purely elastic scattering due to immobile species, and  $y(Q)$  accounts for the quasielastic contribution to the scattering signal from the mobile water molecules. The term  $y(Q)$  is proportional to the elastic incoherent structure factor. For the time intervals longer than 1 ps, the latter was proposed to be equal to  $\exp(-Q^2 a^2/3)$ , where  $a$  describes the root-mean-square vibrational amplitude of a water molecule in the “cage” formed by the neighboring water molecules, in which the water molecule is constrained during its short-time movements.<sup>12</sup> Due to the coupling with the fraction of the elastic scattering, the functional  $Q$  dependence of the elastic incoherent structure factor could be extracted only after the subtraction of the elastic signal from the data. However, we opted not to do so because determining the exact fraction of OH/ $\text{H}_2\text{O}$  species immobile on the time scale of the experiment versus mobile  $\text{H}_2\text{O}$  molecules is difficult. For example, evacuation of the sample even at room temperature may lead to the elimination of not only mobile  $\text{H}_2\text{O}$  molecules but also some surface OH groups that are immobile on the time scale of the backscattering spectrometer, thus yielding incorrectly measured background. Therefore, the meaningful parameters in our analysis were  $x$ ,  $\beta$ , and  $\tau$ .

A stretched exponential relaxation function with  $0 < \beta < 1$  is often used to analyze QENS or neutron spin-echo spectra of supercooled water in confinement.<sup>12–15</sup> The model described by Eq. (1) assumes that on the time scale of the experiment there is only one diffusion component with a distribution of the relaxation times. Similar to the case of surface water in  $\text{ZrO}_2$ , the use of Eq. (1) for  $\text{CeO}_2$  can be justified on the basis that (1) the QENS broadening due to

TABLE I.  $Q$ -averaged fractions of elastic scattering  $x$ , stretch factors  $\beta$ , and the residence times obtained from fitting the inverse average relaxation time in the energy units,  $\Delta E = \hbar / \langle \tau \rangle$ , with Eq. (3). Standard deviation values are shown in parentheses.

$T$ (K)	$\langle x \rangle$	$\langle \beta \rangle$	$\tau_{\text{res}}$ (ps)
250	0.49 (0.001)	0.97 (0.01)	421 (7)
240	0.47 (0.001)	0.96 (0.01)	473 (6)
230	0.46 (0.002)	0.96 (0.01)	551 (13)
220	0.50 (0.002)	0.94 (0.01)	701 (20)
210	0.58 (0.004)	0.93 (0.01)	848 (25)
200	0.69 (0.004)	0.93 (0.02)	865 (49)

the translational dynamics of the outer hydration layer becomes too fast for the dynamic range of the backscattering spectrometer beyond the low- $Q$  range, which is not analyzed in the present work, and (2) the rotational diffusion component also remains very fast compared to the dynamic range of the spectrometer. It should be noted that omitting the low- $Q$  portion of the data does not compromise the accuracy of the determination of the residence time, which depends on the high- $Q$  portion of the data.

The values of the stretch factors obtained from fitting the data with Eq. (1) exhibit a remarkably low scatter through the whole analyzed  $Q$  range suggesting that universal  $Q$ -independent values of  $\beta$  can be used for the data fitting. Such averaged values calculated as  $\langle \beta \rangle = \Sigma(\beta_i / \sigma_i^2) / \Sigma(1 / \sigma_i^2)$  are listed in Table I along with the averaged values of the elastic-scattering fraction,  $\langle x \rangle = \Sigma(x_i / \sigma_i^2) / \Sigma(1 / \sigma_i^2)$ . In agreement with the appearance of the raw data in Fig. 1, the temperature dependence of the elastic-scattering fraction shows an increase below 220 K. With similar areal densities for all the water layers, the outer and inner hydration layers should comprise about 40% of the hydrogen atoms each, and the layer of surface hydroxyl groups should account for about 20% of the hydrogen atoms. The dynamics of the outer layer is too fast and only contributes to the background. Thus, if all the water molecules of the inner hydration layer contribute to the quasielastic signal, one would expect to observe the fraction of the elastic scattering of about 1/3 due to immobile OH groups. The fact that  $x \geq 1/2$  suggests that either not all the molecules of the inner hydration layer are mobile on the time scale of the backscattering spectrometer or the areal density of the molecular water is somewhat smaller compared to that of surface hydroxyl groups.

The stretch factors presented in Table I are close to unity, indicating almost a Debye-type dynamics of the surface water. Nevertheless, we have repeated the fitting with Eq. (1) using the fixed averaged values of beta to obtain the new set of values for the parameter  $\tau$  with reduced standard deviations and then calculated the  $Q$  dependence of the average relaxation time

$$\langle \tau \rangle = \int_0^\infty \exp \left[ - \left( \frac{t}{\tau} \right)^\beta \right] dt = \frac{\tau}{\beta} \Gamma \left( \frac{1}{\beta} \right), \quad (2)$$

where  $\Gamma$  is the gamma function. As we have discussed in the earlier work,<sup>4</sup> a two- rather than three-dimensional character of the surface diffusion does not affect significantly the val-

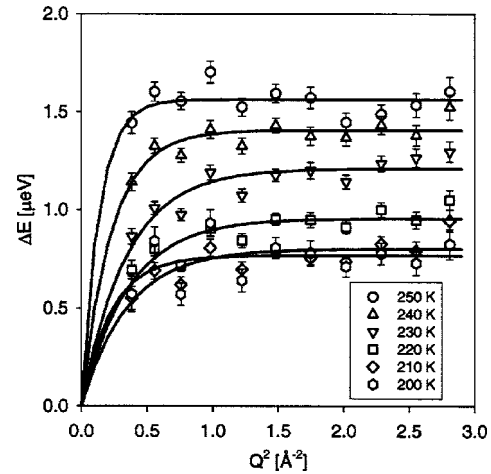


FIG. 2. The  $Q$  dependence of the inverse average relaxation time in the energy units,  $\Delta E = \hbar / \langle \tau \rangle$ , and its fitting using Eq. (3).

ues of  $\beta$  determined from fitting with stretched exponential relaxation functions.

Figure 2 shows the inverse average relaxation time in the energy units,  $\Delta E = \hbar / \langle \tau \rangle$ , plotted as a function of  $Q^2$  and fitted with the expression for a jump diffusion process with a Gaussian distribution of jump lengths<sup>16</sup>

$$\Delta E = \frac{\hbar}{\langle \tau \rangle} = \frac{h}{\tau_{\text{res}}} [1 - \exp(-Q^2 \langle r^2 \rangle / 6)], \quad (3)$$

where  $\langle r^2 \rangle$  is the mean-squared jump distance, and  $\tau_{\text{res}}$  is the residence time between jumps. The residence times obtained from the fitting with Eq. (3) are listed in Table I, and Fig. 3 shows the temperature dependence of  $\tau_{\text{res}}$ .<sup>17</sup> A Vogel-Fulcher-Tamman (VFT) law,  $\tau = \tau_0 \exp(DT_0 / (T - T_0))$ , fits the data points at 250, 240, 230, and 220 K, yielding the glass transition temperature  $T_0 = 181 \pm 3$  K. The VFT fit deviates dramatically from the data at 210 and 200 K, where one can see a sudden change in the slope of the  $1/T$  dependence of  $\log(\tau_{\text{res}})$ . An Arrhenius fit of these two points yields a low

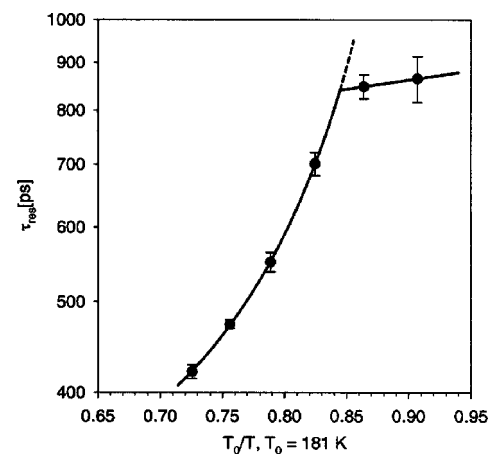


FIG. 3. The temperature dependence of the residence time for the translational diffusion component plotted using  $\log(\tau_{\text{res}})$  vs  $T_0/T$  scale ( $T_0 = 181$  K) and its fits with a VFT law,  $\tau = \tau_0 \exp(DT_0 / (T - T_0))$ , above and an Arrhenius law,  $\tau = \tau_0 \exp(E_A / RT)$ , below the crossover at 215 K. The dashed line shows the extrapolation of the VFT fitting into the lower-temperature region.

activation energy of 0.7 kJ/mol. Similar deviation from a VFT law indicated a fragile-to-strong liquid transition in deeply supercooled confined water.<sup>8</sup> Thus, we interpret this abrupt change in the temperature dependence of the residence time as an indication of a fragile-to-strong liquid transition in surface water that occurs at about 215 K as determined from the intersection of the VFT and Arrhenius fits.

One may argue that the observed deviation from the VFT law might be an artifact due to a limited instrument resolution that was insufficient to capture the longer residence times at low temperatures. At the first sight, this argument could be plausible because of the increasing elastic-scattering fraction. In the case of a distribution of relaxation times, this might indicate that the longer-time part of the distribution cannot be resolved and contributes to the elastic line, thus effectively decreasing the average time of the remaining part of the distribution compared to the average time that would be observed in an ideal experiment with infinitely high resolution. However, this objection can be refuted as follows. The extrapolation of the VFT fit yields the expected values  $\tau_{\text{res}}(210 \text{ K})=1052 \text{ ps}$  and  $\tau_{\text{res}}(200 \text{ K})=2444 \text{ ps}$ . Because the stretch factors are close to unity, translational jump diffusion processes characterized by these residence times would manifest themselves in almost Lorentzian quasielastic broadening in the energy space with the full width at half maximum (FWHM) (evaluated as  $\hbar/\tau_{\text{res}}$  at high  $Q$ ) of  $\approx 1.25 \mu\text{eV}$  at 210 K and  $\approx 0.54 \mu\text{eV}$  at 200 K. Thus, even at 200 K such QENS signal is comparable to the resolution and should still be measurable, whereas at 210 K its width would be well above the instrument resolution of  $0.85 \mu\text{eV}$  (FWHM). Therefore, the change in the temperature dependence of the residence time observed at 210 and 200 K is not an artifact. The increase of the elastic-scattering fraction is also real and is probably related to structural changes in water that accompany fragile-to-strong transition.

Finally, we have repeated the analysis presented in Fig. 3 with the residence times obtained using the simplest model: the  $Q$  dependence of a single Lorentzian model broadening in the energy space fitted with Eq. (3). This represents a jump diffusion process with a distribution of jump lengths and a well-defined time between jumps,  $\tau_{\text{res}}$ . For the temperature dependence of  $\tau_{\text{res}}$  obtained in this way, the VFT fit of the data points at 250, 240, 230, and 220 K yields the glass transition temperature of  $172 \pm 9 \text{ K}$ , the Arrhenius fit of the points at 210 and 200 K yields the activation energy of 0.5 kJ/mol, and the crossover between the two regimes still occurs at 215 K, thus reinforcing our confidence in the robustness of the data analysis that we carried out in the time space.

#### IV. CONCLUSION

The dynamics of surface water in cerium oxide in the temperature range of 200–250 K has been studied in a QENS experiment performed on a backscattering spectrometer with sub- $\mu\text{eV}$  resolution. The slow translational motion of the water molecules in contact with the surface hydroxyl

groups is almost Debye type since its relaxation function can be described by a slightly stretched exponential with the stretch factors exceeding 0.9. Down to  $\approx 220 \text{ K}$ , the temperature dependence of the residence time for the surface water molecules follows a VFT law with the glass transition temperature of 181 K. For comparison, our earlier study yielded the stretch factors between 0.8 and 0.9 for the relaxation functions describing the dynamics of surface water in  $\text{ZrO}_2$  in the measured temperature range of 240–300 K, and its glass transition temperature obtained from a VFT fit was 189 K.<sup>4</sup> In the present study, the temperature dependence of the residence time has been found to deviate dramatically from a VFT law below 220 K. The Arrhenius fit of the data points at 210 and 200 K yielded a low activation energy of 0.7 kJ/mol, and the crossover between VFT and Arrhenius regimes was observed at 215 K. We interpret this crossover as an indication of a fragile-to-strong transition in the surface water, similar to the one recently observed in a QENS measurement of supercooled water confined in a matrix with three-dimensional pores.<sup>8</sup>

#### ACKNOWLEDGMENTS

The author is indebted to Professor S.-H. Chen for a valuable discussion, and to W. Kamitakahara and V. Garcia Sakai for critical reading of the manuscript. Utilization of the DAVE package for the data analysis is acknowledged. This work utilized facilities supported in part by the National Science Foundation under Agreement No. DMR-0086210.

<sup>1</sup>Y. Kuroda, S. Kittaka, S. Takahara, T. Yamaguchi, and M.-C. Bellissent-Funel, *J. Phys. Chem. B* **103**, 11064 (1999).

<sup>2</sup>S. Takahara, S. Kittaka, T. Mori, Y. Kuroda, T. Yamaguchi, and K. Shibata, *J. Phys. Chem. B* **106**, 5689 (2002).

<sup>3</sup>E. Mamontov, *J. Chem. Phys.* **121**, 9087 (2004).

<sup>4</sup>E. Mamontov, *J. Chem. Phys.* **123**, 024706 (2005).

<sup>5</sup>A. Laachir, V. Perrichon, A. Badri *et al.*, *J. Chem. Soc., Faraday Trans.* **87**, 1601 (1991).

<sup>6</sup>G. Gerrato, S. Bordiga, S. Barbera, and C. Morterra, *Surf. Sci.* **377–379**, 50 (1997).

<sup>7</sup>M. Daturi, E. Finocchio, C. Binet, J.-C. Lavalley, F. Fally, and V. Perrichon, *J. Phys. Chem. B* **103**, 4884 (1999).

<sup>8</sup>A. Faraone, L. Liu, C.-Y. Mou, C.-W. Yen, and S.-H. Chen, *J. Chem. Phys.* **121**, 10843 (2004).

<sup>9</sup>K. Ito, C. T. Moynihan, and C. A. Angell, *Nature (London)* **398**, 492 (1999).

<sup>10</sup>H. Knözinger, in *The Hydrogen Bond: Recent Developments in Theory and Experiments*, edited by P. Schuster, G. Zundel, and C. Sandorfy (North-Holland, Amsterdam, 1976), p. 1263.

<sup>11</sup>A. Meyer, R. M. Dimeo, P. M. Gehring, and D. A. Neumann, *Rev. Sci. Instrum.* **74**, 2759 (2003).

<sup>12</sup>J.-M. Zanotti, M.-C. Bellissent-Funel, and S. H. Chen, *Phys. Rev. E* **59**, 3084 (1999).

<sup>13</sup>J. Swenson, R. Bergman, and S. Longeville, *J. Chem. Phys.* **115**, 11299 (2001).

<sup>14</sup>F. Mansour, R. M. Dimeo, and H. Peemoeller, *Phys. Rev. E* **66**, 041307 (2002).

<sup>15</sup>L. Liu, A. Faraone, C.-Y. Mou, C.-W. Yen, and S.-H. Chen, *J. Phys.: Condens. Matter* **16**, S5403 (2004).

<sup>16</sup>P. L. Hall and D. K. Ross, *Mol. Phys.* **42**, 673 (1981).

<sup>17</sup>Unlike  $\tau_{\text{res}}$ , which is defined by the quasielastic broadening measured at larger  $Q$  values, the mean-squared jump distance is determined from the data at low- $Q$  values. The absence of the low- $Q$  data in our analysis leads to very large errors in  $\langle r^2 \rangle$ , which makes the values of  $\langle r^2 \rangle$  determined from the fitting highly unreliable.